Computer Simulation of Semidilute Polymer Solutions in Confined Geometry: Pore as a Microscopic Probe

Yongmei Wang*

Department of Chemistry, North Carolina A & T State University, Greensboro, North Carolina 27411

Iwao Teraoka

Department of Chemical Engineering, Chemistry, and Materials Science, Polytechnic University, 333 Jay Street, Brooklyn, New York 11201

Received May 28, 1997; Revised Manuscript Received September 15, 1997[⊗]

ABSTRACT: We present a lattice computer simulation study on the geometrical confinement effect of polymer solutions in a wide range of concentrations. Polymer chains were equilibrated for a system that consists of a bulk solution and a slit between two parallel walls. The partition coefficient of the polymer was determined and found to increase as the bulk concentration ϕ increased, confirming the theoretical predictions. We applied the blob picture to analyze the partition coefficient data in the semidilute regime where the partitioning is considered to be controlled by the ratio of the blob size to the slit width, rather than by the ratio of the chain dimension to the slit width. Our simulation data and earlier experimental data support the application of the blob theory. Furthermore, we found it is possible to estimate the blob size in the bulk solution directly from the partition coefficient data by assuming that the confinement entropy of the blob depends on the blob size in the same way as the confinement entropy of the individual chain depends on the chain dimension at infinite dilution. The blob size thus determined confirms the scaling prediction; namely, the blob size $\propto \phi^{-3/4}$. Some deviations from this simple picture, however, exist when the slit is narrow and the solution is concentrated.

Introduction

Partitioning of polymers between a confined geometry and a bulk solution is a fundamental issue[1,2] in applications such as size exclusion chromatography (SEC).[3] Past efforts have been predominantly made in studies of the partitioning of polymers at infinite dilution,[2] partly because SEC operates in this condition. However, the partitioning of polymers at semidilute and high concentrations is worthy of detailed examination for two reasons. First, the newly developed technique known as high osmotic pressure chromatography (HOPC)[4−6] makes use of partitioning at high concentrations to fractionate polydisperse polymer samples. This technique provides an efficient and cost-effective way to prepare polymer fractions with narrow molecular weight distributions. A better understanding of the partitioning at high concentrations is key to the development of HOPC. Second, a porous medium can be used as a probe of microscopic length in polymer solutions. De Gennes proposed a blob picture[1] to describe semidilute polymer solutions. The blob picture has been successfully used to explain many phenomena of such solutions. Several studies have tried to confirm the blob picture. Neutron scattering[7] and light scattering[8] have been used to examine the blob size (correlation length). Computer simulations[9] and osmometry[10] also confirmed the blob picture. All of these studies confirmed the crossover from an isolated chain to a blob in the motional units of the system. We will show in this report that the partitioning of polymer between a confined geometry and a semidilute solution also shows the crossover from the partitioning of isolated chains to that of blobs.

We performed lattice Monte Carlo simulations of linear chain molecules partitioning into a slit for a wide range of concentrations and different slit widths. Simulation data on the partitioning of polymers that covers dilute to semidilute solutions are limited in the literature. Bleha et al.,[11] for instance, conducted simulations for a cubic pore, but the concentrations were not sufficiently high to reach the semidilute regime. In the off-lattice simulations for the partitioning of tetramers and octamers into a slit by Yethiraj and Hall,[12] the oligomers were not solvated (the meaning will be explained later). Thompson and Glandt[13] performed simulations for long chains. The porous medium examined was a quenched deposition of nonoverlaping hard spheres. The partition coefficient showed a diffuse transition from a weak penetration (exclusion of long chains by the pore) to a strong penetration (the polymer concentration in the pore becomes nearly equal to the one in the surrounding solution because of high osmotic pressure). However, with the poorly defined pore geometry, the data from their simulations cannot be analyzed by the blob picture. Our lattice simulation covers dilute to semidilute regimes and employs a well-defined pore geometry (slit). This advantage enables us to examine the data in the light of the blob picture.

Simulation Models

Our simulation model is similar to the model used by Yethiraj and Hall,[12] except that we use a lattice simulation. The lattice simulation is faster and more efficient than the off-lattice simulation, and therefore we can examine longer chains and a wider range of concentrations. The simulation box (see Figure 1) has two regions connected to each other: region E, representing the exterior bulk phase, and region I, representing the interior pore channel. Region E is a tetragonal box with dimensions of $L_a \times L_b \times L_c$, where L_a, L_b, and L_c are the lengths along x, y, and z directions, respectively. Region I is also tetragonal with dimensions of $L_x \times L_y \times L_z$ ($L_y = L_b$). There are two solid walls extending in the y and z directions. No polymer beads

[⊗] Abstract published in *Advance ACS Abstracts,* December 15, 1997.

S0024-9297(97)00741-9 CCC: $14.00

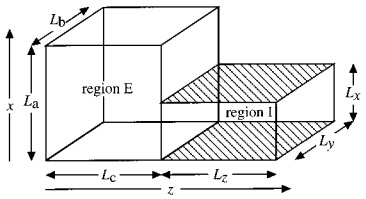

Figure 1. Schematic of the simulation box.

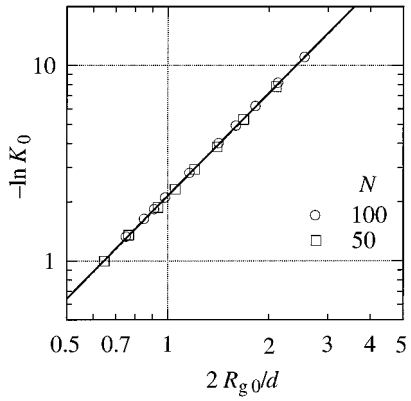

Figure 2. Plot of $-\ln K_0$ as a function of $2R_{g0}/d$. The straight line is the best fit by a power law.

Table 1. Polymer Chains Used in the Simulations

N	R_{g0}	ϕ^*
50	4.212	0.2366
100	6.377	0.1363

may occupy the sites on these walls. The distance between the two walls can be varied to represent different widths of the pore channel. Periodic boundary conditions (PBC) are applied in all of the three directions except where the walls are. The PBC along the z direction has subtle variations. For layers with $1 \le x \le L_x - 1$, the periodic boundaries are layers $z = 1$ and $z = L_c + L_z$. For $L_x \le x < L_a - 1$, however, they are at $z = 1$ and $z = L_c$. With walls at $x = 1$ and $x = L_x$, there are $L_x - 2$ layers reserved for polymer beads. The slit width d is then given as $d = L_x - 1$.

The polymer chains are represented by self-avoiding walks of length N on the simple cubic lattice. The system is equilibrated by using reptation moves with the Metropolis rule.[14] Table 1 shows the lengths of the chains used in the simulations, their root-mean-square radii of gyration, R_{g0}, in the dilute solution limit, and the overlap concentrations ϕ^* defined as $\phi^* \equiv N(\sqrt{2}R_{g0})^{-3}$. Typically a box of $30 \times 30 \times 50$ was used for region E, and region I was a box of $L_x \times 30 \times 50$ with $L_x = 8$, 10, 12, 15, and 18. The partition coefficient K is given by $K = \phi_I/\phi_E$, where ϕ_E is the average concentration of the polymer beads in the exterior region E, and ϕ_I is average concentration in region I. The simulation time depends on the chain length and the box size. Typically the simulation was run for a sufficiently long time so that the density profile in region E has fluctuations of no more than 0.5%. A typical error bar in the partition coefficinet K is <1%.

To determine the partition coefficient K_0 in the dilute solution limit, we used the Rosenbluth-Rosenbluth Monte Carlo method.[11,15] Figure 2 shows a plot of $-\ln K_0$ as a function of $2R_{g0}/d$. Note that $\ln K_0 = \Delta S/k_B$, where ΔS is the change in the conformational entropy of an isolated chain upon being transferred into the pore, and k_B is the Boltzmann constant. Results obtained for the two different chain lengths and various

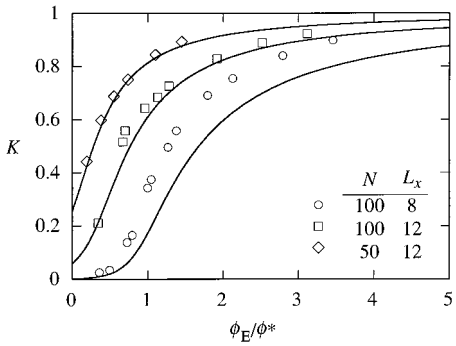

Figure 3. Typical simulation results. The partition coefficient K is plotted as a function of the exterior concentration ϕ_E, reduced by the overlap concentration ϕ^*, for three series of simulations. The simulation conditions are indicated in the figure. Calculation results are shown for comparison (solid lines).

slit widths are on a single straight line. The line represents a fitting of $-\ln K_0$ by $b(2R_{g0}/d)^\alpha$, with adjustable parameters b and α. The best fitting resulted in $b = 2.1548$ and $\alpha = 1.7479$. Our α is slightly larger than the one predicted ($5/3$[1] or $1/0.588$[16]). The power law was originally derived by using the scaling theory for strongly excluded chains (i.e., those with $R_{g0} \gg d$[1]). Some of the data in the figure do not satisfy that condition. This situation may have contributed to the larger exponent observed. What is important here, however, is that the confinement entropy for a chain on the lattice by a slit is given as $-\Delta S/k_B = b(2R_{g0}/d)^\alpha$.

Simulation Results

Typical simulation results are shown in Figure 3. The partition coefficient K is plotted as a function of the reduced concentration in the exterior solution. The K increased as ϕ_E increased, in agreement with theoretical predictions[17,18] of the weak-to-strong penetration transition. The solid line represents a theoretical calculation that we obtained using the theory of Teraoka et al.[18] A few assumptions used in the theory are (1) the concentration in the slit is uniform (no depletion layer), (2) the osmotic pressure of the solution in the slit is a function of ϕ_I and is equal to the osmotic pressure of the bulk solution at the same concentration, (3) the chain contraction factor in the slit (before the confinement affects it) is the same as the one in the bulk solution of the same concentration, and (4) the confinement entropy of a chain of dimension R_g (after contraction) is given as $-\Delta S/k_B = b(2R_g/d)^\alpha$. The formulas for the osmotic pressure and the chain contraction factor were derived by Ohta and Oono.[19]

The theoretical partitioning curve fits the simulation data well when the slit is sufficiently wide ($L_x \ge 12$). For $L_x = 8$, however, polymer chains penetrated the pore more easily than the calculation shows. We first speculated that the first assumption just mentioned caused the error. To take into account a nonuniform distribution of the concentration in the slit, we assumed that the concentration profile follows that of a Gaussian chain.[20] The result was not much different from what is shown in Figure 3, and actually produced a line that lies slightly below the curve in the figure. The deviation is therefore not due to the neglect of the intrapore distribution of the polymer beads. This finding led us to believe that the second assumption is not correct. We speculated as follows. The second virial coefficient in the virial expansion with respect to the volume fraction is smaller in the two-dimensional imperfect gas (inter-

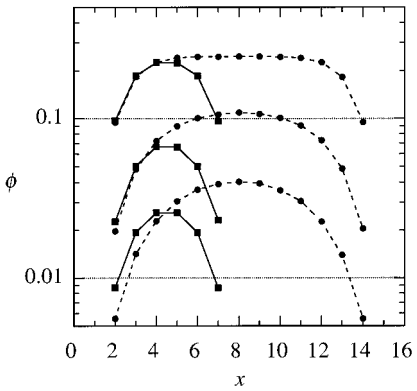

Figure 4. Concentration profile across the slit for $L_x = 8$ (solid line) and 15 (dashed line) at three pairs of concentrations (from bottom to top, respectively, $\phi_E = 0.1080$, 0.1724, and 0.244 for $L_x = 8$, and $\phi_E = 0.0562$, 0.1122, and 0.2433 for $L_x = 15$).

actions are excluded-volume only) compared with the three-dimensional counterpart. The interaction is weaker if molecules are allowed to interact with neighboring molecules in a reduced number of dimensions, and should be so at higher concentrations as well. Weaker interactions in the pore will bring in more polymer chains, which is why the agreement is good when the slit is wide and the interior solution is close to that in the three-dimensions, but is bad when the slit imposes a strong confinement to render two-dimensional characteristics in the intrapore solution, (i.e., congested pancakes).[17] At this moment, we do not have an explicit expression of the interation that takes into account this effect.

In all of the simulations, we also calculated the profile of monomer concentration ϕ across the pore space. Some of the profiles are shown in Figure 4 for $L_x = 8$ and 15. Three pairs of concentrations ($\phi_E = 0.1080$, 0.1724, and 0.244 for $L_x = 8$, and $\phi_E = 0.0562$, 0.1122, and 0.2433 for $L_x = 15$) were selected to provide nearly matching interior concentrations. The walls are at $x = 1$ and 8 for $L_x = 8$, and at $x = 1$ and 15 for $L_x = 15$. At low concentrations, the profiles for the two slit widths almost overlap, when ϕ, normalized by the value at the slit center, is plotted as a function of $(x - 1)/d$ (not shown), except that the profile for the narrower slit is a coarse-grained version of the other profile. This feature is in agreement with the theoretical result that the fundamental mode with a wavelength $2d$ dominates[1,20] when the chain dimension is not too small compared with d. As ϕ_E increases, the profile for $L_x = 15$ becomes flatter around the mid plane of the slit, and the concentration of the flat portion is almost identical with ϕ_E. The depletion layer becomes thinner. It is interesting to see that the profile for $L_x = 8$ follows that of $L_x = 15$ at $x = 2$, 3, and 4. The features at high concentrations agree with what we expect for the partitioning of a solute with a dimension sufficiently smaller than $L_x = 15$. Apparently, these polymer chains are partitioned as if they were a solute of a smaller dimension.

Unlike results obtained in off-lattice simulations for hard-sphere chains in vacuum,[12] we did not observe the ordering of beads near the walls at high concentrations. The absence of ordering is because of discretization of the space in our lattice Monte Carlo simulations.[21] The polymer chains behave as chains solvated in an athermal solvent in lattice simulations because empty lattice sites serve as sites occupied by the solvent. This situation is in contrast to the off-lattice simulations in

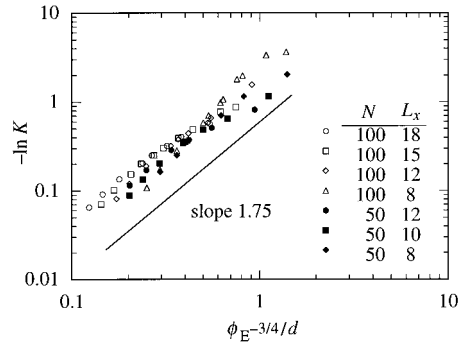

Figure 5. Plot of $-\ln K$ as a function of $\phi_E^{-3/4}/d$ for all the simulation results obtained. The straight line has a slope of 1.75.

which the unoccupied continuum space is not equivalent to the space occupied by solvent. An illustrative example is given by considering the effect of walls in an off-lattice simulation that explicitly includes polymer chains and monomeric solvent particles at real liquid density. The solvent particles will be enriched near the wall because they experience a smaller loss of entropy compared with that experienced by polymer chains near the wall. Hence, the volume fraction of the polymer segments over the total particle densities, equivalent to the density profile obtained in the lattice simulation, will not exhibit the ordering effect. In the absence of the momomeric solvent particles in the off-lattice simulations, however, packing of the hard sphere oligomers near the wall causes the ordering effect as observed in the previous studies by Yethiraj and Hall.[12]

Transition from Partitioning of a Whole Chain to That of a Blob

In the dilute solution, each polymer chain with a typical dimension of R_{g0} is moving independently. As the concentration ϕ increases and exceeds the overlap concentration, the motional unit changes to a blob. The semidilute solution can be considered to consist of closely packed blobs.[1] The dimension ξ of a blob is given as $\xi \sim R_{g0}(\phi/\phi^*)^{-3/4} \sim \phi^{-3/4}$, and is equal to the correlation length of the monomer density. The crossover of the motional unit from individual chains to blobs has been confirmed in a few different types of experiments. In the osmometry[10] that essentially counts the number of moving units, it was confirmed that the osmotic pressure Π reduced by thermal energy k_BT follows $\Pi/(k_BT) \sim \xi^{-3}$. In the static light scattering,[8] the correlation length ξ was found to depend on ϕ as predicted, and the osmotic compressibility $(\partial\Pi/\partial\phi)_T$ scaled as $(\phi/\phi^*)^{5/4}$. In the dynamic light scattering,[22] the dynamic correlation length of the concentration fluctuations was found to scale as $\phi^{-3/4}$. In computer simulations,[9] it was found that the cutoff length, beyond which the excluded volume effect is shielded, scaled as $\phi^{-3/4}$.

The partitioning of polymer in semidilute solutions may also be discussed in the blob picture. At low concentrations, polymer chains with $R_{g0} \gg d$ find it difficult to enter the pore. As the concentrations exceeds ϕ^*, the motional unit changes to a blob whose dimension decreases as ϕ increases. Thus, the chains can penetrate the pore more easily. The partition coefficient should be determined by ξ/d, as opposed to R_{g0}/d at infinite dilution. This picture is another view of the transition from weak penetration to strong penetration.[1] Our picture is supported by Figure 5 in which $-\ln K$, obtained in simulations for different chain lengths, slit

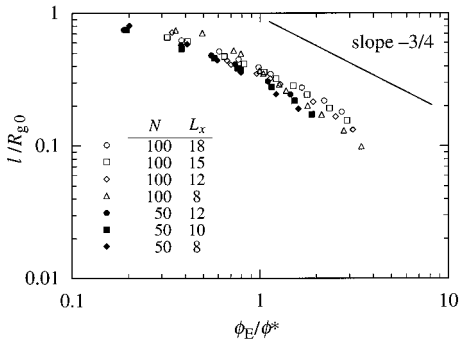

Figure 6. Reduced length of a motional unit, l/R_{g0}, is plotted as a function of ϕ_E/ϕ^* for all the simulation results obtained. The straight line has a slope of −3/4.

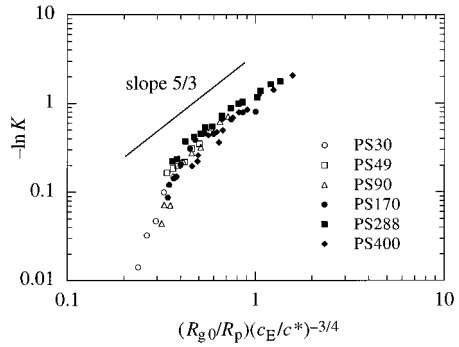

Figure 7. Confinement entropy −ln K, obtained in the interferometry, is plotted as a function of the ratio of the correlation length $R_{g0}(c_E/c^*)^{-3/4}$ to the pore radius R_p. The straight line has a slope of 5/3.

widths, and concentrations, is plotted as a function of $\phi_E^{-3/4}/d$. The data for $N = 100$ and $N = 50$ are plotted as open and closed symbols, respectively. A large difference in K between different simulation conditions is mostly removed, and the data points appear to lie along a master curve except for low concentrations.

Nevertheless, $\xi \sim \phi^{-3/4}$ is only an estimation of the blob size based on the scaling theory. It is valid only in the semidilute regime, and the exact numerical factor is not known. A more direct estimation of the actual length of the motional unit can be obtained as follows. First, we note that the plot of −ln K versus $\phi_E^{-3/4}/d$ in Figure 5 exhibits the same power-law dependence as the one we saw in Figure 2 for the plot of −ln K_0 versus $2R_{g0}/d$. This coincidence is not too surprising because, as the blob theory predicts, both blobs and individual chains should be partitioned according to the same size exclusion principle; that is, the free energy of confining a blob is similar to that of confining a single chain of the same dimension. Then it may be possible to estimate the size l of the motional unit from the value of K obtained at each concentration by using the formula, $-\ln K = b(2l/d)^{\alpha}$ (b and α were obtained in Figure 2). The l represents the size, as probed by the slit, of independently moving units that constitute the exterior solution. Figure 6 is a plot of the resulting l/R_{g0} as a function of ϕ_E/ϕ^*. The straight line in the figure has a slope of −3/4 as predicted by the scaling theory. The plot shows that there is a crossover in the motional unit from an isolated chain to the blob as the exterior solution becomes semidilute. In the range of $0.6 < \phi_E/\phi^* < 2$ for $N = 100$ and $0.6 < \phi_E/\phi^* < 1$ for $N = 50$ (note a narrow range of the semidilute solution for the latter), the data points are parallel to the line, and the blob size is now responsible, in the crude approximation, for the partitioning. The points for $N = 50$ are somewhat lower, a result we ascribe to the difference in the actual chain length (or chain of blobs). This figure compares well with the plots of the correlation length obtained in the static and dynamic light scattering.[8,22] The transition in the concentration profile in the pore we saw in Figure 4 is also a result of the change in the motional unit.

At higher concentrations (so-called concentrated regime), the data points fall below the line of slope −3/4 that could be drawn to fit the points in the semidilute regime. This result may indicate that l falls off more rapidly in the concentrated regime. The latter suggestion, however, needs more studies because, in our simulations, l in that range is <1.0 (the lattice spacing) as opposed to $1.3 \lesssim l \lesssim 3.2$ in the semidilute regime.

Here we will use the scaling theory[1] to show that the partitioning depends on ξ/d at high concentrations. The chemical potential μ_E of a polymer chain in a solution of concentration ϕ_E is expressed as follows:

$$\mu_E/k_BT \cong \mu_0/k_BT + \ln \phi_E + (\phi_E/\phi^*)^{5/4} \qquad (1)$$

where μ_0 refers to a reference state. In a solution of concentration ϕ_I within a slit of width d, the chemical potential μ_I is given as follows:

$$\mu_I/k_BT \cong \mu_0/k_BT + \ln \phi_I + (\phi_I/\phi^*)^{5/4} + (R_{g0}/d)^{5/3} \qquad (2)$$

where the effect of the chain contraction is not taken into account because the effect was smaller compared with the effect of the third term.[18] At low concentrations (i.e., ϕ_E, $\phi_I \ll \phi^*$), $\mu_E = \mu_I$ leads to the following scaling result:

$$-\ln K = -\ln (\phi_I/\phi_E) \cong (R_{g0}/d)^{5/3} \qquad (3)$$

At sufficiently high concentrations, the interaction term dominates the chemical potential, and therefore ln ϕ terms can be dropped from eqs 1 and 2. Then, from $\mu_E = \mu_I$, we have the following:

$$-\ln K \cong -\ln [1 - (R_{g0}/d)^{5/3}(\phi_E/\phi^*)^{-5/4}] \cong (\xi/d)^{5/3} \qquad (4)$$

where $\xi \sim R_{g0}(\phi_E/\phi^*)^{-3/4}$ was used. From comparison of eqs 3 and 4, we find that the partitioning shows a crossover from that of a single chain of size R_{g0} at low concentrations to that of a blob of size ξ at high concentrations.

We are now tempted to reexamine existing experimental data in the light of the crossover. The data obtained by Teraoka[23] using Jamin interferometry is the only set that covers a semidilute range. Partition coefficient data compiled from the measurements for six different molar masses of polystyrene with a porous silica bead of pore radius $R_p = 25$ nm are shown in Figure 7. Only the data in the range of $c_E/c^* > 0.5$ are shown as a function of $(R_{g0}/R_p)(c_E/c^*)^{-3/4}$, where c_E is the concentration of the polystyrene fraction in the exterior solution, and c^* is its overlap concentration defined in the same way as ϕ^* was defined. The abscissa is the ratio of the correlation length to the pore radius. The straight line represents a prediction of the blob theory and has a slope of 5/3. All the points except for short chains at high concentrations appear to run parallel to the straight line. The figure shows that the partitioning of the semidilute solution is equivalent to that of suspensions of radius $\xi \sim R_{g0}(c_E/c^*)^{-3/4}$. A difficulty of

estimating K_0 does not allow us to prepare a plot for the length of the motional unit, however.

Concluding Remarks

We have shown in this report that the partitioning of polymer chains in semidilute solutions is governed by the size of the motional unit in the solution relative to the pore size. By simply replacing the chain dimension by the blob size, the partitioning rule that is valid at low concentrations applies to semidilute solutions as well. Thus, a pore can be used as a microscopic probe to explore structures in solution systems. Small systematic deviations from the rule are observed. Those deviations between chains of different lengths may be due to the connectivity of blobs in the same chain. We cannot discuss the deviations at high concentrations because in that range, the length of the motional unit is less than the lattice spacing. Simulations for longer chains will help resolve the issues.

References and Notes

(1) de Gennes, P.-G. *Scaling Concepts in Polymer Physics*; Cornell University: Ithaca, NY 1979.
(2) Teraoka, I. *Prog. Polym. Sci.* **1996**, *21*, 89.
(3) Yau, W. W.; Kirkland, J. J.; Bly, D. D. *Size-exclusion liquid chromatography*; Winefordner, J. D., Ed.; John Wiley: New York, 1989; Vol. 98, pp 277−316.
(4) Luo, M.; Teraoka, I. *Macromolecules* **1996**, *29*, 4226.
(5) Luo, M.; Teraoka, I. *Polymer*, in press.
(6) Teraoka, I.; Luo, M. *Trends Polym. Sci.* **1997**, *5*, 258.
(7) Daoud, M.; Cotton, J. P.; Farnoux, B.; Jannink, G.; Sarma, G.; Benoit, H.; Duplessix, R.; Picot, C.; de Gennes, P. G. *Macromolecules* **1975**, *8*, 804.
(8) Wiltzius, P.; Haller, H. R.; Cannel, D. S. *Phys. Rev. Lett.* **1983**, *51*, 1183.
(9) Paul, W.; Binder, K.; Heermann, D. W.; Kremer, K. *J. Phys. II (Paris)* **1991**, *1*, 37.
(10) Noda, I.; Kato, N.; Kitano, T.; Nagasawa, M. *Macromolecules* **1981**, *14*, 668.
(11) Bleha, T.; Cifra, P.; Karasz, F. E. *Polymer* **1990**, *31*, 1321.
(12) Yethiraj, A.; Hall, C. K. *Mol. Phys.* **1991**, *73*, 503.
(13) Thompson, A. P.; Glandt, E. D. *Macromolecules* **1996**, *29*, 4314.
(14) Metropolis, N.; Rosenbluth, A. W.; Rosenbluth, M. N.; Teller, A. H.; Teller, E. *J. Chem. Phys.* **1953**, *21*, 1087.
(15) Cifra, P.; Bleha, T.; Romanov, A. *Makromol. Chem., Rapid Commun.* **1988**, *9*, 355.
(16) des Cloizeaux, J.; Jannink, G. *Polymers in Solution: Their Modelling and Structure*; Clarendon: Oxford, 1990.
(17) Daoud, M.; de Gennes, P. G. *J. Phys. (Paris)* **1977**, *38*, 85.
(18) Teraoka, I.; Langley, K. H.; Karasz, F. E. *Macromolecules* **1993**, *26*, 287.
(19) Ohta, T.; Oono, Y. *Phys. Lett.* **1982**, *89A*, 460.
(20) Casassa, E. F.; Tagami, Y. *Macromolecules* **1969**, *2*, 14.
(21) Binder, K. *Physica A* **1993**, *200*, 722.
(22) Schaefer, D. W.; Han, C. C. *Quasielastic light scattering from dilute and semidilute polymer solutions*; Plenum: New York, 1985.
(23) Teraoka, I. *Macromolecules* **1996**, *29*, 2430.

MA970741T